



7-9 February, 2012

THEME: Geo-Budget: Enabling Sustainable Growth

Mineral Abundance Mapping Using Hyperion Dataset in Part of Udaipur Dist Rajasthan, India

Salaj.S.S¹, RichaUpadhyay², Dr.S.K.Srivastav³, Dr.Prabhakaran⁴

^{1,4} PSNA College of Engineering and Technology, Dindigul

^{2,3} Indian Institute of Remote Sensing, Dehradun

E-mail: salaj2067@gmail.com

Abstract

Satellite-based hyperspectral imaging became a reality in November 2000 with the successful launch and operation of the Hyperion system on board the EO-1 platform. The product is distributed by USGS, and the level one product, which is only radiometrically corrected, is used. Hyperspectral remote sensing has the potential to provide the detailed physico-chemistry (mineralogy, chemistry, morphology) of the earth's surface. The present study attempts to test the abilities of Hyperion data for mineral abundance mapping in the study area comprising part of Udaipur Dist, Rajasthan. Pre-processing requirements to prepare high quality data for analysis purposes then performed on data. In this study, FLAASH software was used to convert radiance into corresponding reflectance. Due to the low reflectance level in some bands, the original 196 bands were reduced to 144 bands after the atmospheric correction. A minimum noise fraction (MNF) transformation was used to reduce the dimensionality of the hyperspectral data by segregating the noise in the data. The Pixel Purity Index (PPI) was computed by continually projecting n-dimensional scatterplots onto a random vector. N-Dimensional visualization techniques were used to select endmembers within a scene. Four endmembers were collected from the Udaipur study area and they are Grossularite, Pyrite, Calcite and Andradite. Endmembers identified by PPI and N-dimensional visualizer are compared spectrally to the United States Geological Survey (USGS) mineral spectral library. Mixture Tune Matched Filtering and Spectral Angle Mapper (SAM) were applied to estimate abundances of each endmember to produce final map. Mixture Tune Matched Filtering gave good results in mapping the endmembers while SAM has given intermixing of endmembers in study area. In conclusion, it can be said that the low signal to noise ratio of Hyperion and presence of smile effect in the image and the use of laboratory spectra of these minerals from the standard spectral libraries as the reference affected the classification results and their accuracies.

1. Introduction

The hyperspectral sensors represent one of the most important technological trends in remote sensing which combines imaging and spectroscopy in a single system, includes datasets composed of large (about 100 to 200) spectral bands of relatively narrow bandwidths(5-20 nm). Hyperspectral remote sensing, measuring hundreds of spectral bands from aircraft and satellite platforms, provides unique spatial/spectral datasets for analysis of surface mineralogy (Goetz et al., 1985; Kruse et al.,2003). These data allow mapping of key iron mineralogy such as hematite, goethite, and jarosite as well as alteration minerals such as kaolinite, dickite, alunite, and sericite (Clark et al., 1990). Their use for geologic applications is well established (Goetz et al., 1985; Kruse et al., 1999,2003; Rowan and Mars, 2003).

As part of the US New Millennium Program (faster, cheaper, better), the launch of the EO-1 satellite platform in November 2000 introduced hyperspectral sensing of the Earth from space through its Hyperion system (Pearlman,et al., 1999 and Liao et al., 2000) albeit as a scientific experiment. The EO-1 has a sun-synchronous orbit with an altitude of 705 km and a 10:01 AM descending node The orbit inclination is 98.2 degree. Equatorial crossing time is one minute behind Landsat-7.The telescope provides for two separate grating image spectrometers to improve signal-to-noise ratio(SNR).The Hyperion VNIR sensor has 70 bands(355.589-851.92nm), and the SWIR has 172 bands(1057.36-2577.07nm) providing 242 potential bands.Different mineral have a unique reflectance and absorption pattern across different wave-length. So, minerals can be uniquely identified. Two main causes for the absorption features are : i) Electric Processes and ii) Vibrational Processes. Hyperion uses two atmospheric windows, the VNIR & SWIR regions for mapping surface mineralogy because these wave-lengths are sensitive to a wide range of diagnostic EMR-material interactions.

The primary aims and objectives of the present work is to understand EO-1 Hyperion data processing and spectral analysis for mineral abundance mapping in part of Udaipur dist,Rajasthan and to find greater application of hyperspectral remote sensing techniques in mineral exploration. This study attempts to map the various minerals present in the exposed rock surface in the study area.

2. Study Area

The study area is a part of Udaipur District, Rajasthan, India. The area is located southwest of Udaipur City covering a part of Hindustan Zinc Limited – Zawar Mines area. The extent of the study area is from 73° 33' 25" E to 73° 42' 53" E and 24° 09' 34" N to 24° 31' 40" N covering 303.43 sq km. Udaipur District is one of the 33 districts of Rajasthan state in western India. Udaipur District is bounded on the northwest by the Aravalli Range, across which lie the districts of Sirohi and Pali.The Udaipur city of Rajasthan comes under the semi-arid terrain with negligible amount of vegetation.Geologically the region comes under the Pre-Cambrian era of the geological time scale.

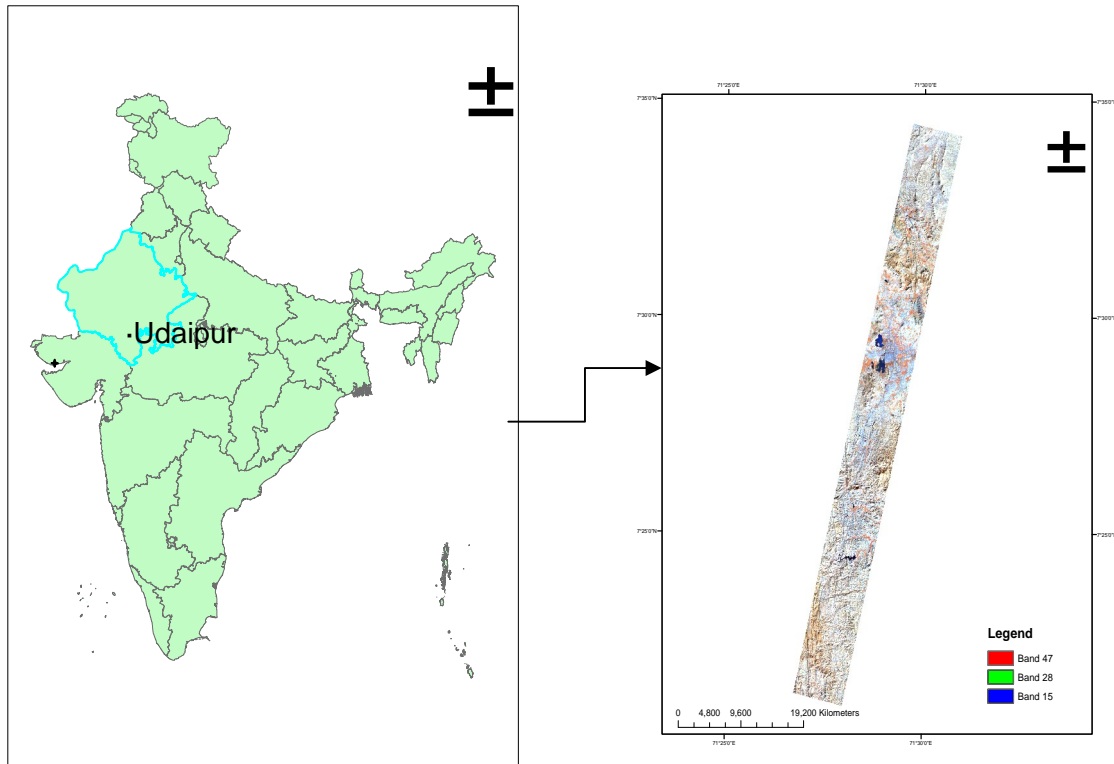


Figure 1- Study area (Udaipur), Hyperion (FCC 47 28 15)

2.1 Geological setting

The geological setting of Udaipur area is not only unique in the state but also shows wide complexity. It is considered as one of the “type area” of the Aravali Super group of rock. The study area broadly has two main stratigraphic units i.e. rocks of Aravali Supergroup and pre-Aravali Formations. Aravali Supergroup of rocks around Udaipur city shows a high degree of structural complexity and polyphase deformation history. However at some places (near Fatehsagar) the graywacke and phyllite rocks are not metamorphosed or deformed and display some typical sedimentary characters like ripple marks, mud cracks, rain prints etc.

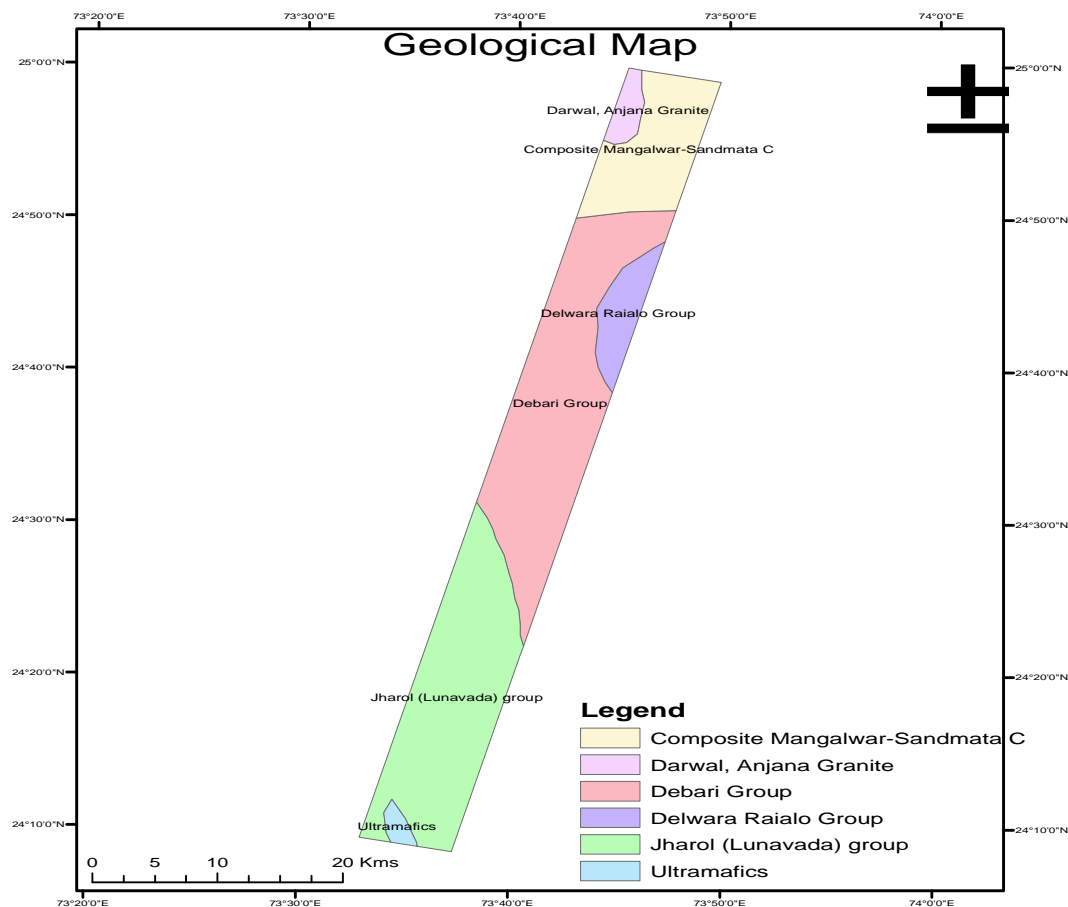


Figure 2-Geological map of Udaipur study area Modified after S.Sinha-Roy et al

Banded Gneissic Complex

The Banded Gneissic Complex (BGC) in Rajasthan can be divided into three major rock groups, i.e. Mangalwar complex, Sandmata Complex and the Hindoli Group. The BGC in Udaipur and its surroundings can be grouped under the Mangalwar and the Sandmata Complex. The mangalwar complex is a heterogeneous assemblage of amphibolite-facies metamorphites comprising of migmatites, composite gneisses, feldsparitic mica schist, sillimanite-kyanite-mica-schist, hornblende schist, granite gneiss and amphibolite along with minor carbonates constitute the Mangalwar complex (Gupta et.al. 1981). The Sandmata Complex are the high-grade metamorphites, comprising of migmatites, composite gneisses, biotite-schist, garnet-sillimanite-staurolite-biotite schist, dolomitic marble, hornblende schist with associated granite, are included in the Sandmata complex. The boundary between the Sandmata Complex and the Mangalwar Complex is marked by isograd roughly along the Delwara Lineament. Sinha-Roy et al. (1992) suggested that the Sandmata Complex constitutes only the high pressure granulite facies rocks having tectonic contact with the encompassing Mangalwar complex rocks.

The Aravalli Supergroup can be divided into two principal facies sequences. One is the Delwara group which is volcanic dominated and the volcanics free Debari Group. The Delwara group occupies the lowermost position in the Aravalli stratigraphy. It comprises of mafic volcanics, clean-washed quartzite, quartz pebble conglomerate (QPC), minor carbonates and

BIF. The lithoassemblage comprising coarse clastics, carbonates and pelites constitute the Middle Aravalli sequence and is designated as the Debari Group (Sinha-Roy et al,1993b). The carbonate free and pelite dominant sequence with arenite bands constitute a large part of the Aravalli sequence and it is named as the Jharol Group (Gupta et al, 1981). It is interpreted as distal turbidities or flysch of the Aravalli deepsea sequence. The rock sequence comprising of coarse pelitic schist and quartzite with phosphoritic dolomite that occur in a roughly polygonal area in southern Rajasthan is referred to as Lunavada Group. Ultramafic rocks represented by serpentinite, talc-tremolite schist, antigorite-tremolite schist and monomineralic chloro-schist occur along two regional lineaments, i.e. Rakhabdev Lineament in the east and Kaliguman Lineament in the west (Bakliwal and Ramaswamy,1987). Although these bodies occur as lenses and linear bands of variable dimensions, their disposition marks a linearity. These Ultramafic rocks were variably described as ‘Magnesian rocks’ (Middlemiss, 1921) and as ‘talc-serpentine-chlorite rock’(Ghosh,1933). Based on the field and petrochemical studies (Gathania et al., 1995) divided the Ultramafics into three groups; the first group consisting of coarse grained carbonate-talc dominated rock occurring near the contact with the metasediments, while the second group consists of dark coloured antigorite-chlorite bearing rocks, while monomineralic chlorite rich forms the third group. The latter occurs as intrusive bodies within other ultramafic groups and metasediments. The above mentioned facts regarding the geologic setting of Udaipur study area have been referred from “Geology of Rajasthan” by S. Sinha-Roy, G. Malhotra and M. Mohanty, Geological Society of India, Bangalore, 1988.

3. Data Used & Methodology

The following data was used for the study

- 1) Hyperion Level 1R and Level 1Gst images
- 2) Geological Map of the Study Area (Figure-2)
- 3) Spectral Library (USGS)

Hyperion data onboard EO-1 satellite acquired on 19.01.2004 is used for this study. The product is distributed by USGS, and the Hyperion Level 1R data, which is only radiometrically corrected is used for the current study. Hyperion collects 242 unique spectral channels ranging from 0.357 to 2.576 micrometers with a 10-11 nm bandwidth. Level 1Gst dataset is radiometrically and geometrically corrected data. It is also terrain corrected. This dataset is having same details as level1R data. It was used for geometric correction of L1R data. The overall methodology which was adopted for this study was illustrated in the **Figure 3**.

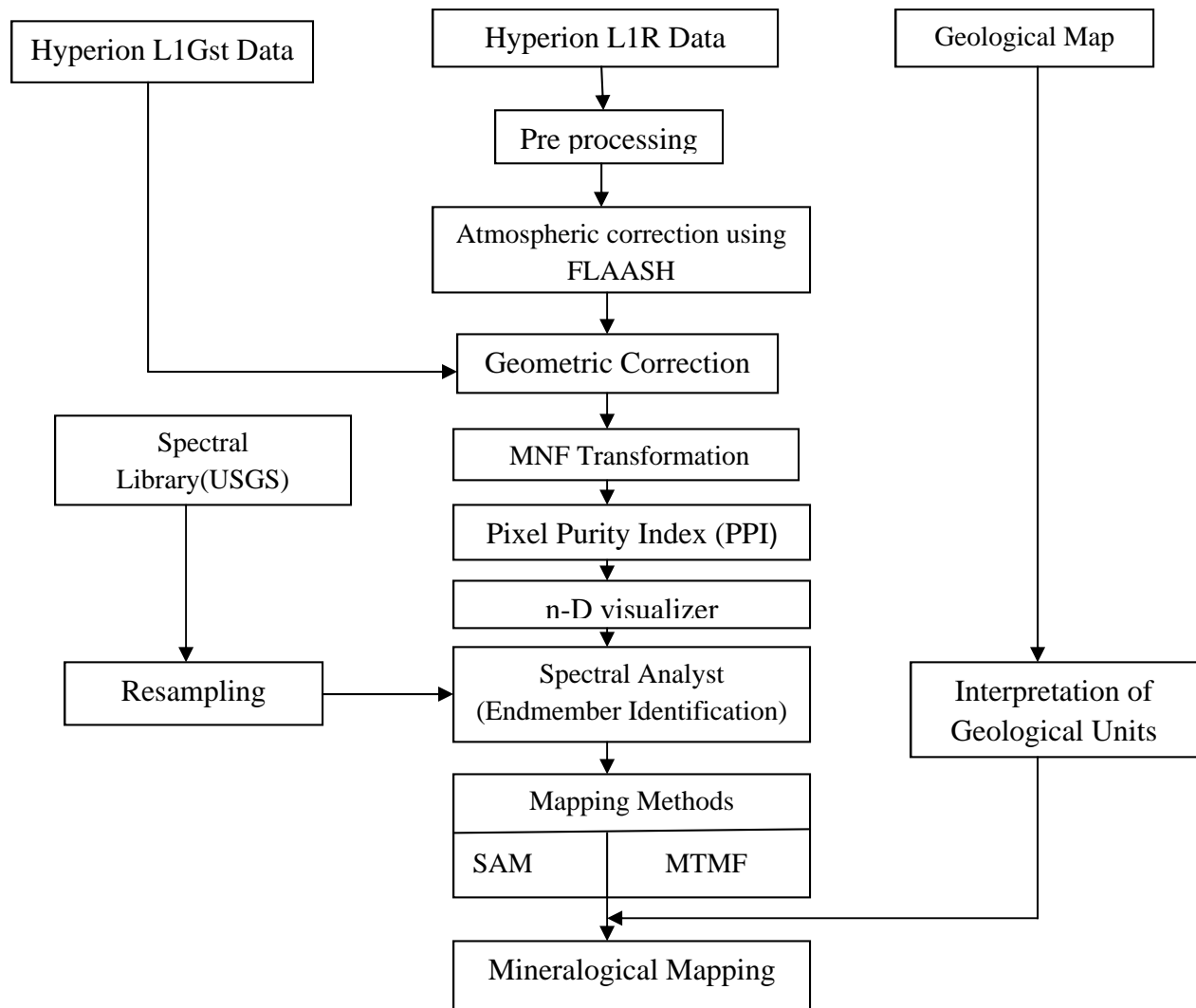


Figure 3 - The Flow Diagram of Methodology

4. Data Pre-Processing

Hyperspectral data poses challenges to image interpretation, because of high data volume, redundancy in information, need for calibration, and dimensionality problem. The raw Hyperion image is having certain errors arising due to atmosphere or malfunctioning of sensor mechanism. The errors are said to be caused due to calibration differences in the detector array (Goodenough et al., 2003). Some of the bands, particularly in lower and upper ends of the spectral range exhibit poor signal to noise ratio. As a result, during level 1 processing, only 198 bands are calibrated. The apparent strips are frequently found in several bands. To reduce the errors caused by the stripping effect, all spectral bands are screened and manually rejected a total of 54 bands with apparent stripping effects from VNIR + SWIR spectral range. A spatial subset was taken to focus on the study area.

4.1 Correction for Bad Columns

The raw image has some dark and bright columns occurring due to change in the calibration or failure of some detectors in the CCD array at the time of capturing the image. The scan line

dropout or stripping errors should be removed before atmospheric corrections. The bad columns were replaced by taking average of the previous and next column.

4.2 Atmospheric Correction using FLAASH Module

Solar radiation is affected by its path through the atmospheric absorption and scattered in the combined Sun-surface-sensor. The radiance obtained by a sensor is modified by the atmosphere as well as by the Earth's surface. Because of this, spectral imagery includes information about the atmosphere and the earth's surface. Atmospheric correction (or compensation) of spectral imagery refers to the retrieval of surface reflectance spectra from measured radiances. Spectral imagery of the Earth's surface from airborne or space platforms can be used to fullest advantage only when the effects of the atmosphere (e.g., from aerosol, water vapour, etc.) have been removed and the data are reduced to units of reflectance. In collaboration with the Air Force Research Laboratory and other US Government agencies, SSI has developed a state-of-the-art, first-principles atmospheric removal (or "correction") algorithm called FLAASH (Fast Line-of-sight Atmospheric Analysis of Spectral Hypercubes). FLAASH handles data from a variety of HSI and MSI sensors, supports off-nadir as well as nadir viewing, and incorporates algorithms for water vapour and aerosol retrieval and adjacency effect correction (Matthew et al., 2000).

FLAASH requires the input radiance image containing calibrated radiance data in a floating point, long integer (4-byte signed), or integer (2-byte signed or unsigned) data type having units $W/cm^2 * nm * steradian$. The image should have BIL or BIP format. To convert the raw image into radiance units all the VNIR bands should be divided by a scale factor 40 and the SWIR bands by 80. For inputting the image in FLAASH those bands should be divided by 400.0 and 800.0 respectively. A text file containing array of 400.0 for first 70 VNIR bands and 800.0 for the 172 SWIR bands was created and used at the time of inputting the image in FLAASH.

5. Hyperspectral Analysis

The following procedures of hyperspectral analysis were employed, including the Minimum Noise Fraction (MNF) transformation for reducing spectral data, the Pixel Purity Index (PPI) for identifying those extreme or spectrally pure pixels, and the n-Dimensional Visualizer for determining the endmember directly from the image. Mixture Tune Matched Filtering and Spectral Angle Mapper (SAM) were applied to estimate abundances of each endmember to produce final map.

5.1 Minimum Noise Fraction

The minimum noise fraction (MNF) transformation determines the inherent dimensionality of image data, to segregate noise in the data, and to reduce the computational requirements for subsequent processing. This is a two step process. The first step results in transformed data in which the noise has unit variance and no band-to-band correlations. The second step is a standard Principal Components transformation of the noise-whitened data.

5.2 Pixel Purity Index (PPI)

The Pixel Purity Index (PPI) is a means of finding the most “spectrally pure,” or extreme, pixels in multispectral and hyperspectral images (Boardman et al., 1995). The most spectrally pure pixels typically correspond to mixing endmembers. PPI is computed by repeatedly projecting n-dimensional (n-D) scatter plots onto a random unit vector. ENVI records the extreme pixels in each projection are recorded—those pixels that fall onto the ends of the unit vector and it notes the total number of times each pixel is marked as extreme. A PPI image is created where each pixel value corresponds to the number of times that pixel was recorded as extreme. The PPI is typically run on an MNF transform result; excluding the noise bands. PPI was calculated with 10000 iterations and a threshold factor in the data unit was set to 2.5 for extreme pixel selection. The results of the PPI are used as input into n-D Visualizer.

5.3. The n-Dimensional Visualizer

To further refine the selection of the most spectrally pure end members from the derived two dimensional PPI image and more importantly, to label them with specific end member types (i.e., to assign these end members to specific mineral types), it is essential to re-examine visually the selected pixels in the n-dimensional feature space and to assign them manually to appropriate types (Boardman and Kruse, 1994). The selected classes were exported to Region of Interest (ROI) and used as input for further spectral processing.

5.4. Spectral Angle Mapping

Spectral angle mapper (SAM) is a procedure that determines the similarity between a pixel and each of the reference spectra based on the calculation of the “spectral angle” between them (Boardman and Kruse, 1994). This method treats both (the questioned and known) spectra as vectors and calculates the spectral angle between them (Figure 4). It works on images with apparent reflectance and determines the similarity between two spectra by calculating the “spectral angle” between them, treating them as vectors in a space with dimensionality equal to the number of bands. A smaller angle means a closer match between the two spectra and the pixel is identified as the fixed class. SAM determines the similarity of an unknown spectrum t to a reference spectrum r , by applying the following equation.

$$\alpha = \cos^{-1} \left[\frac{\bar{t} * \bar{r}}{\|\bar{t}\| * \|\bar{r}\|} \right] \quad (1)$$

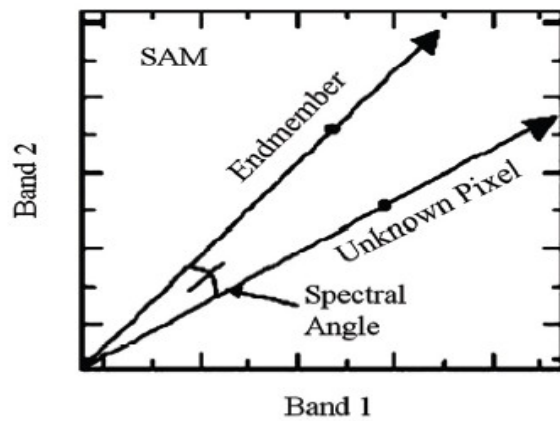


Figure 4 showing the SAM algorithm

5.5 Mixture Tuned Matched Filtering

Matched Filtering removes the requirement of knowing all of the endmembers by maximizing the response of a known endmember and suppressing the response of the composite unknown background, thus matching the known signature (Chen and Reed, 1987; Stocker *et al.*, 1990; Yu *et al.*, 1993; Harsanyi and Chang, 1994). It provides a rapid means of detecting specific minerals based on matches to specific library or image endmember spectra. This technique produces images similar to the unmixing, but with significantly less computation and without the requirement to know all the endmembers. Mixture-Tuned Matched Filtering (MTMF) is a hybrid method based on the combination of well-known signal processing methodologies and linear mixture theory (Boardman, 1998). This method combines the strength of the Matched Filter method (no requirement to know all the endmembers) with physical constraints imposed by mixing theory (the signature at any given pixel is a linear combination of the individual components contained in that pixel). MTMF uses linear spectral mixing theory to constrain the result to feasible mixtures and to reduce false alarm rates (Boardman, 1998).

6. Results & Discussion

The forward MNF transformation was performed on 144 bands of preprocessed image to reduce the dimensionality of the data. The first eight eigenbands were selected containing most of the spectral information. Therefore, they were used to determine the pure pixels in the Hyperion image using PPI procedure. PPI was calculated with 10000 iterations and a threshold factor of 2.5 for extreme pixel selection. From the PPI image, the purest pixels were selected by giving a threshold of 200. A total of 460 pixels were shortlisted and converted to Region of Interest. These pixels were used for further processing. The spectra of pure pixels were plot into an n-dimensional scatter plot to determine the endmembers. The resampled USGS mineral library is used through spectral analyst to identify the material of the endmembers extracted from N-D Visualizer. The Spectral Angle Mapper and Spectral Feature Fitting techniques were used for the identification. Equal weightage was given to both the techniques and the mineral with maximum score for matching was identified as the material for that endmember. The pixel clusters for each material were refined and finalized by checking spectral profiles of each and every pixel in the cluster. Finally four minerals were identified through the process and they are Grossularite, Pyrite, Calcite and Andradite. The spectral profiles of the endmember minerals were used for abundance mapping are shown in the following figure-5.

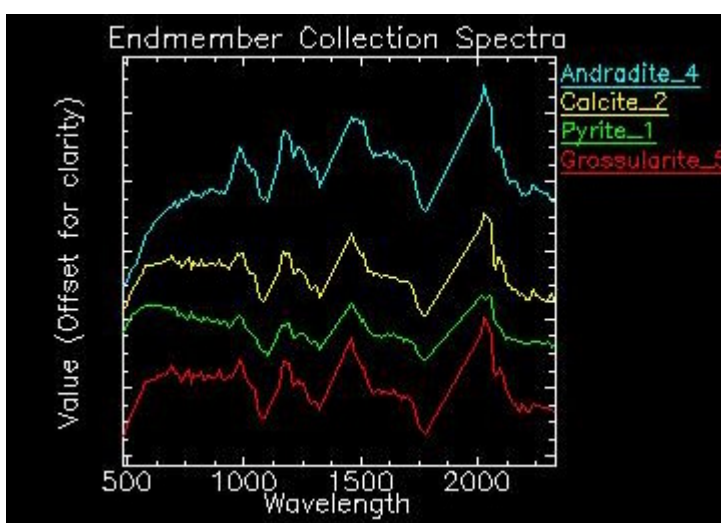
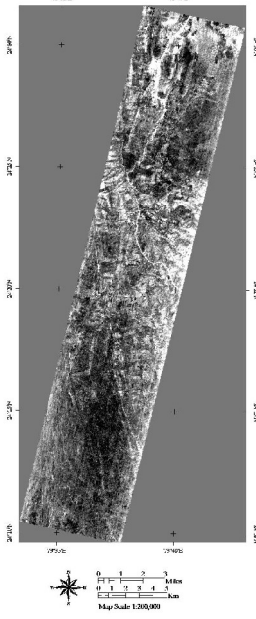


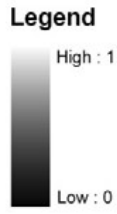
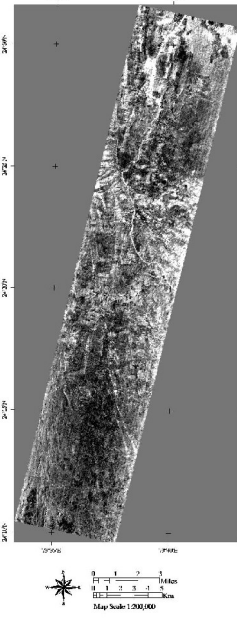
Figure-5 Spectral profiles of Endmembers

Mixture Tune Matched Filtering and Spectral Angle Mapper (SAM) were applied to estimate abundances of each endmember to produce final map. Mixture Tune Matched Filtering gave good results in mapping the endmembers while SAM has given intermixing of endmembers in study area. The mineral abundance map of each endmembers is shown in the figure-6

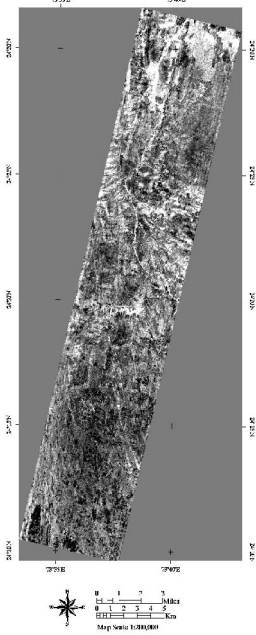
Grossularite



Calcite



Pyrite



Andradite

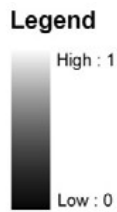
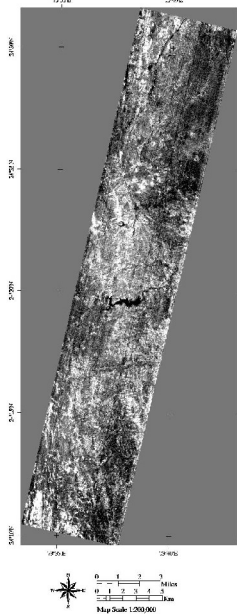
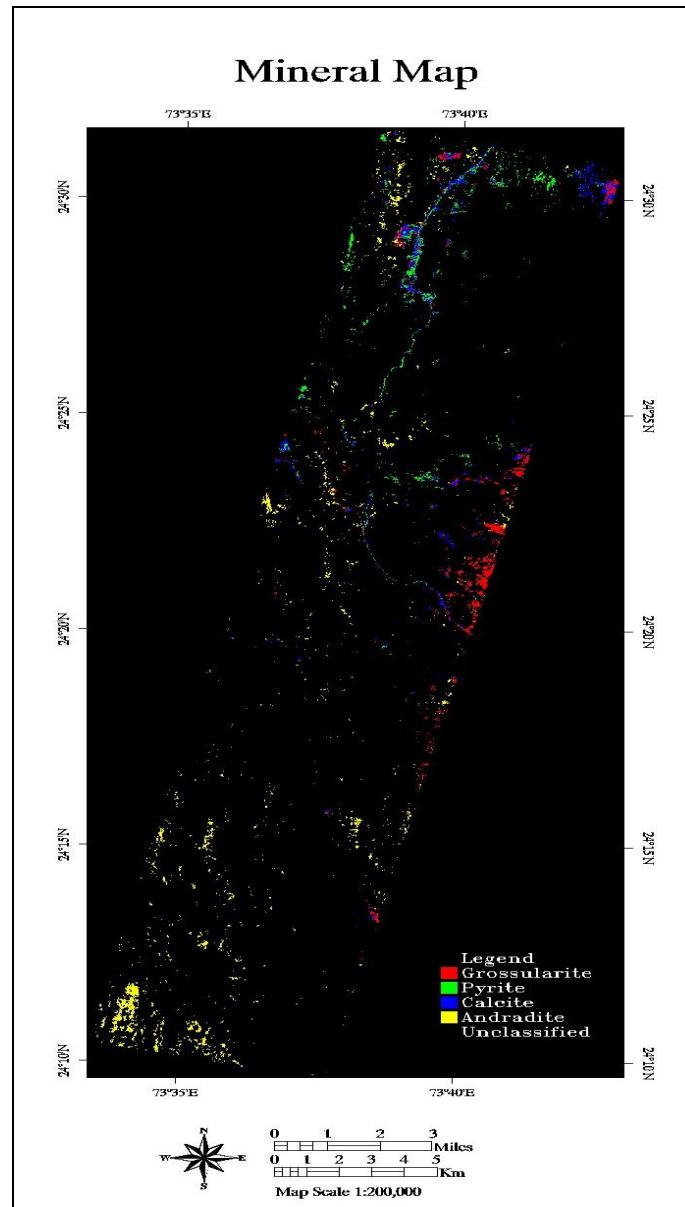


Figure-6 Mineral abundance maps for Grossularite,Calcite,Pyrite,Andradite

To locate the best places for each mineral, a combined map was prepared using rule classifier wherein threshold values of each end members was used. The final mineralogical map created from the abundance maps using Rule Classifier is shown in the figure-7.



Topography, vegetation along with the use of reference spectra from the standard spectral libraries which differ to a large extent from the spectra of actual minerals in the field conditions, has led to some amount of misclassification. Hence the output mineral map shows many 'false positives' along with the correct results.

7. Conclusion

The study illustrates that Hyperion data is useful for identifying mineral abundances and mapping the geological characteristics. Minerals identified are in accordance with the ground lithology, but the spatial distribution of those minerals in the map is affected by topographic disturbances and presence of vegetation. In conclusion, it can be said that the low signal to noise ratio of Hyperion and presence of smile effect in the image and the use of laboratory spectra of these minerals from the standard spectral libraries as the reference affected the classification results and their accuracies.

9. References

- Bakliwal, P.C. and Ramasamy, S. M. (1987). Lineament fabric of Rajasthan and Gujarat, India, *Rec. Geol. Surv. Ind.*, v.113 (7), pp. 54-64.
- Beck, R., 2003. EO-1 User Guide, Version: 2.3. USGS Earth resources Observation systems Data Center (EDC).
- Boardman J. W., and Kruse, F. A., 1994, Automated spectral analysis: A geologic example using AVIRIS data, north Grapevine Mountains, Nevada: in *Proceedings, Tenth Thematic Conference on Geologic Remote Sensing*, Environmental Research Institute of Michigan, Ann Arbor, MI, p. I-407 - I-418.
- Boardman, J. W., 1998, Leveraging the high dimensionality of AVIRIS data for improved sub-pixel target unmixing and rejection of false positives: mixture tuned matched filtering, in: *Summaries of the Seventh Annual JPL Airborne Geoscience Workshop*, Pasadena, CA, p. 55.
- Boardman, J. W., Kruse, F. A., and Green, R. O., 1995, Mapping target signatures via partial unmixing of AVIRIS data: in *Summaries, Fifth JPL Airborne Earth Science Workshop*, JPL Publication 95-1, v. 1, p. 23-26.
- Chen, J. Y., and I. S. Reed, 1987, A detection algorithm for optical targets in clutter, *IEEE Trans. on Aerosp. Electron. Syst.*, vol. AES-23, no. 1.
- Clark, R.N., T.V.V. King, M. Klejwa And G.A. Swayze (1990): High spectral resolution spectroscopy of minerals, *J. Geophys. Res.*, 95 (B8), 12653-12680. 92
- ENVI Tutorials," Research Systems, Inc., Boulder, 2002
- Gathania, R.C et al. (1995). Occurrence of ultramafics of komatiitic affinity in the Rakhabdev-Dungarpur belt, Udaipur and Dungarpur Dists. Rajasthan, *Jour. Geol. Soc. Ind.* V.46, pp.585-594.
- Ghosh, P.K. (1933). Talc-serpentine-chlorite rocks of southern Mewar and Dungarpur, *Rec. Geol. Surv. Ind.* V. LXVI(4).
- Goodenough, G.D., Dyk, A., Niemann, O.K. and Pearlman, J.S., 2003. Preprocessing Hyperion and ALI for forest classification. *IEEE Transactions on Geoscience and Remote Sensing*, 41(6 Part 1): 1321-1331

Gupta et al. (1981). Lithostratigraphic map of Aravalli region, Southeastern Rajasthan and northern Gujarat, Geol. Surv. Ind., Hyderabad.

Harsanyi, J.C., Chang, C., 1994. Hyperspectral image classification and dimensionality reduction: An Orthogonal subspace projection approach. IEEE Transactions on Geoscience and Remote Sensing 32, 779-785.

Heron, A.M. (1953). The geology of central Rajaputana, Mem. Geol. Surv. Ind., v. 79, pp. 1-389

Kruse, F.A., J.W. Boardman And J.F. Huntington (1999), Fifteen years of hyperspectral data: Northern Grapevine Mountains, Nevada, in Proceedings of the 8th JPL Airborne Earth Science Workshop, Jet Propulsion Laboratory Publ. 99-17, 247-258.

Kruse, F.A., J.W. Boardman And J.F. Huntington (2003): Evaluation and validation of hyperion for mineral mapping, IEEE Trans. Geosci. Remote Sensing, 41 (6), 1388-1400.

L. Liao, P. Jarecke, D. Gleichauf And T. Hedman (2000), "Performance Characterization of the Hyperion Imaging Spectrometer Instrument", Proc. of SPIE, Vol. 4101, pp. 22-26, July 2000.

Matthew, M.W. et al., 2000. Status of atmospheric correction using a MODTRAN4-based algorithm, Algorithms and Technologies for Multispectral, Hyperspectral, and Ultraspectral Imagery VI. SPIE, Orlando, FL, USA.

Middlemiss, C.S. (1921). Geology of Idar state. Mem Geol. Surv. Ind., v. XLIV(1).

Pearlman, J., S. Carman, P. Lee, L. Liao And C. Segal (1999): Hyperion imaging spectrometer on the new millennium program Earth Orbiter-1 system, in Proceedings of the International Symposium on Spectral Sensing Research (ISSSR), Systems and Sensors for the New Millennium, International Society for Photogrammetry and Remote Sensing (ISPRS), (CD-ROM).

Research Systems Inc (RSI), 2001, ENVI User's Guide, Research Systems Inc, 948 p.

Rowan, L.C. And J.C. Mars (2003): Lithologic mapping in the Mountain Pass, California area using Advanced Spaceborne Thermal Emission and Reflection Spectrometer (ASTER) data, Remote Sensing Environ., 84,350-366.

Roy, A.S. (1988). Stratigraphic and tectonic framework of the Aravalli Mountain Range. In : A.B. Roy (Eds.) Precambrians of Aravalli Mountain, Rajasthan, India, Mem. Geol. Soc. Ind., v.7, pp. 3-31.

S Sinha-Roy, G Malhotra, M Mohanty (1998), Geology of Rajasthan, Geological Society of India, 1st edition, 278 p.

Sinha-Roy, S et al. (1993b). Conglomerate horizons in south central Rajasthan and their significance on Proterozoic stratigraphy and tectonics of the Aravalli and Delhi fold belts, Jour. Geol. Soc. Ind., v.41, pp. 331-350.